Research Article Vol. 4, No. 12 / December 2017 / Optica 1462

Generation of the complete four-dimensional Bell basis

Feiran Wang,[1,2,3,†] Manuel Erhard,[1,2,*,†] Amin Babazadeh,[1,2,4] Mehul Malik,[1,2] Mario Krenn,[1,2] and Anton Zeilinger[1,2,5]

[1]Vienna Center for Quantum Science & Technology (VCQ), Faculty of Physics, University of Vienna, Boltzmanngasse 5, 1090 Vienna, Austria
[2]Institute for Quantum Optics and Quantum Information (IQOQI), Austrian Academy of Sciences, Boltzmanngasse 3, 1090 Vienna, Austria
[3]Key Laboratory of Quantum Information and Quantum Optoelectronic Devices, Shaanxi Province, Xi-an Jiaotong University, Xi-an 710049, China
[4]Physics Department, Institute for Advanced Studies in Basic Sciences, Zanjan, Iran
[5]e-mail: anton.zeilinger@univie.ac.at
*Corresponding author: manuel.erhard@univie.ac.at

Received 25 July 2017; revised 27 September 2017; accepted 1 October 2017 (Doc. ID 303015); published 28 November 2017

The Bell basis is a distinctive set of maximally entangled two-particle quantum states that forms the foundation for many quantum protocols such as teleportation, dense coding, and entanglement swapping. While the generation, manipulation, and measurement of two-level quantum states are well understood, the same is not true in higher dimensions. Here we present the experimental generation of a complete set of Bell states in a four-dimensional Hilbert space, comprising 16 orthogonal entangled Bell-like states encoded in the orbital angular momentum of photons. The states are created by the application of generalized high-dimensional Pauli gates on an initial entangled state. Our results pave the way for the application of high-dimensional quantum states in complex quantum protocols such as quantum dense coding.

OCIS codes: (270.0270) Quantum optics; (270.5565) Quantum communications; (270.5568) Quantum cryptography; (270.5585) Quantum information and processing.

https://doi.org/10.1364/OPTICA.4.001462

1. INTRODUCTION

Quantum entanglement is not only a curious phenomenon that radically deviates from our everyday experiences; it is also essential for many quantum information applications. High-dimensional entanglement [1–7] offers specific advantages over qubit entanglement, which is conventionally used in quantum information applications. The use of high-dimensional entanglement can enhance quantum communication schemes by increasing their channel capacity [8,9] and offering improved robustness against sophisticated eavesdropping attacks [10,11]. High-dimensionally entangled states can potentially be used for the teleportation of quantum states of ever-increasing complexity [12]. In addition, such states can enhance the capacity of quantum dense-coding schemes that allow for the sharing of more information than is classically possible [13,14].

Quantum communication schemes such as these usually require control over a basis of maximally entangled quantum states—the so-called *Bell basis*. For example, both quantum teleportation [15] and entanglement swapping [16] require one to unambiguously distinguish between at least one of the Bell states. In quantum dense coding, the generation, manipulation, and discrimination of Bell states is essential, as they form the basis in which information is encoded [14]. Polarization-entangled states have proved to be the most versatile implementation of two-dimensional Bell states thus far, and have found use in several quantum communication protocols. In addition to the polarization degree of freedom, two-dimensional Bell states have also been demonstrated with time-bin entangled states [17] and recently with photons entangled in their orbital angular momentum [18,19].

Here we demonstrate the experimental generation of a complete basis of four-dimensional Bell-like entangled states. Our experiment constitutes the first demonstration to our knowledge of a complete Bell basis beyond qubits. In the case of two-dimensional polarization entanglement, it is well known that one can rotate between all four Bell states with a half-wave plate (which performs a Pauli-X transformation) and a quarter-wave plate (performing a Pauli-Z transformation). We generate all 16 Bell states by generalizing this method to a higher-dimensional Hilbert space.

Our states consist of two photons entangled in their orbital angular momentum (OAM) [20,21]. The 16 orthogonal states in this basis are created by applying high-dimensional generalizations of Pauli gates on an initial OAM-entangled state that is produced via spontaneous parametric down-conversion. A four-dimensional X-gate is applied to one photon of the entangled pair, which corresponds to a cyclic transformation between the four basis states [22–24]. The second photon is sent through a four-dimensional Z-gate, which imparts a mode-dependent

phase shift on the photon. We quantify the quality of our generated states by measuring their overlap with ideal states from a four-dimensional Bell basis and verify the presence of four-dimensional entanglement by measuring an appropriate entanglement witness.

2. TECHNIQUE

The D-dimensional Bell basis of a bipartite system AB, as generalized in the original teleportation paper by Bennett *et al.* [15], can be written in the form

$$|\psi\rangle_{AB}^{mn} = \frac{1}{\sqrt{D}} \sum_{k=0}^{D-1} e^{i\frac{2\pi}{D}nk} |k\rangle_A |k \oplus m\rangle_B, \tag{1}$$

where $k \oplus m \equiv (k+m) \bmod D$. For $D = 2$, this reduces to the four well-known maximally entangled quantum states $|\Psi^{\pm}\rangle$ and $|\Phi^{\pm}\rangle$, which are either symmetric or antisymmetric. In the four-dimensional case, Eq. (1) involves 16 orthogonal Bell states that can be categorized into four distinct groups as shown in Fig. 1(a). The four states in each group are labeled by the variable $n = 0, 1, 2, 3$, which defines the phase relationships between the probability amplitudes. As defined in Eq. (1), the four-dimensional Bell basis contains two antisymmetric and six symmetric states, while the remaining eight states are neither symmetric nor antisymmetric.

In the first set of states ψ_{0n} in Fig. 1(a), photons A and B share the same state, while the relative phase between the probability amplitudes varies according to n. The other three sets of states are obtained by performing specific transformations on the first group. To obtain the second group ψ_{1n}, photon B is transformed using clockwise cyclic mode transformation X ($-2 \to -1 \to 0 \to 1 \to -2$). For the groups ψ_{2n} and ψ_{3n}, the state of photon B is transformed by an X^2 transformation ($-2 \leftrightarrows 0, -1 \leftrightarrows 1$) and an anticlockwise cyclic transformation $X^{\dagger}$ ($-2 \to 1 \to 0 \to -1 \to -2$), respectively. To transform among states within each group, photon A undergoes a mode-dependent phase transformation. In this manner, all 16 states in the four-dimensional Bell basis are obtained (Fig. 1). Since this is a bipartite maximally entangled system, it does not matter on which photon or in which order the phase and cyclic transformations are applied.

3. EXPERIMENT

As shown in Fig. 2, photons entangled in their OAM are generated via a frequency-degenerate type-II spontaneous parametric down-conversion (SPDC) process in a periodically poled potassium titanyl phosphate (ppKTP) crystal. The photons are produced in the state

$$|\Psi\rangle = \sum_{\ell=-\infty}^{+\infty} c_{\ell} |-\ell\rangle_A |\ell\rangle_B, \tag{2}$$

where $|\ell\rangle$ represents a photon carrying an OAM of $\ell\hbar$ and c_{ℓ} is a complex probability amplitude. For the purposes of our experiment, we use a four-dimensional subset of this state consisting of OAM mode values ℓ varying from -2 to 1. One photon is vertically polarized and thus reflected by the polarizing beam splitter (PBS) into path A. The other photon is horizontally polarized and therefore transmitted at the PBS into path B. The reflection at the PBS flips the sign of the OAM mode ($|\ell\rangle \to |-\ell\rangle$). This transforms the entangled photons into the first state of our basis $|\psi_{00}\rangle = (|-2,-2\rangle + |-1,-1\rangle + |0,0\rangle + |1,1\rangle)/2$. In order to create the remaining three states in the first group, we apply a mode-dependent phase transformation with a Dove prism (DP) in arm A. In general, a DP oriented at an angle α introduces a phase $|\ell\rangle \to \exp(i2\ell\alpha)|\ell\rangle$ that depends on the OAM value ℓ of the incoming photon and the rotation angle α of the prism. The effect of this element on the state can be written as

$$|\Psi\rangle \xrightarrow{\mathrm{DP}(\alpha)} |\Psi'\rangle = \frac{1}{2} \sum_{\ell \in \{-2,-1,0,1\}} e^{i2l\alpha} |\ell\rangle_A |\ell\rangle_B. \tag{3}$$

By orienting the DP at different angles ($\alpha = 0, \pi/4, \pi/2, 3\pi/4$), we obtain all four states in one group.

A fourfold clockwise cyclic transformation of OAM modes was recently developed through the use of the computer algorithm Melvin [22] and implemented with coherent light as well as single photons [23,24]. The principle idea of cyclic transformations is to split even and odd OAM modes into two different paths and manipulate them independently. Finally, the two paths are recombined coherently. In our experiment, we implement three such cyclic transformations (X, X^2, $X^{\dagger}$) at the single-photon level.

As shown in Fig. 2, we use a double-path Sagnac interferometer containing two DPs [25] to split even and odd OAM modes into two different paths (green frame). In the path for even OAM modes, different OAM manipulations are performed that are necessary for the three cyclic transformations. The two paths are probabilistically recombined with a beam splitter (BS), forming a Mach–Zehnder (MZ) interferometer. In principle, the two paths can be recombined with another parity sorter in a deterministic way. To perform the X transformation ($-2 \to -1 \to 0 \to 1 \to -2$), a spiral phase plate (SPP) adds an OAM quantum of $+1$ before the OAM sorter. After the sorter,

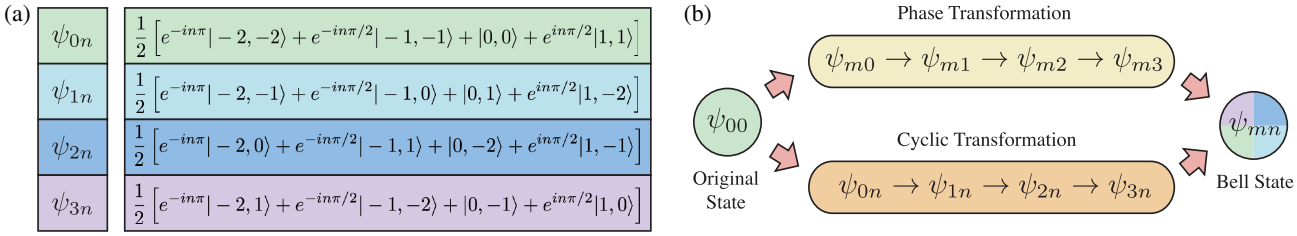

Fig. 1. Generating 16 four-dimensional Bell states. (a) The 16 Bell states can be divided into four classes of four states each. Within each class, the states only differ in mode-dependent phases. States from different classes differ by their OAM number. (b) By employing a mode-dependent phase transformation on photon A and a cyclic mode transformation on photon B, the complete set of 16 maximally entangled four-dimensional Bell states can be obtained.

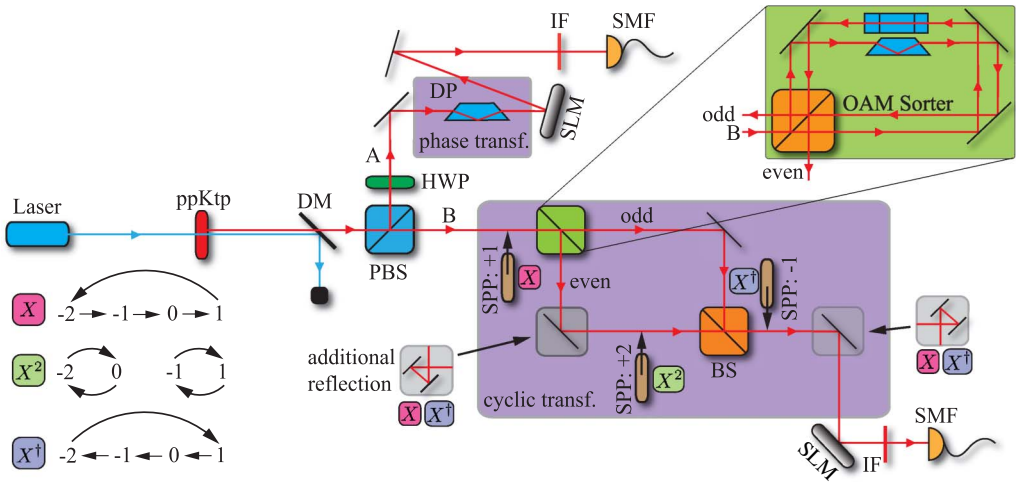

Fig. 2. Experimental setup of 4D Bell states. A laser creates a pair of OAM-entangled photons in a nonlinear crystal (ppKtp) that are deterministically separated with a polarizing beam splitter (PBS). The upper path A includes a Dove prism (DP) that implements mode-dependent phase transformations for different rotation angles. The photons transmitted through the PBS arrive at the OAM sorter (green frame). This sorter contains two DPs with a relative angle of 90°, which results in interference that depends on the parity (odd or even) of the spatial mode. For reasons of stability, the OAM sorter is implemented as a double-path Sagnac interferometer. There, odd modes are transmitted, while even modes are reflected (thus also changing the sign of their OAM). To implement the three cyclic transformations (X, X^2, $X^\dagger$), only a spiral phase plate (SPP) and a mirror have to be installed in different positions. A spatial light modulator (SLM) together with a single mode fiber (SMF) is used to perform projective measurements.

one of the paths of the MZ interferometer undergoes an additional reflection. A final additional reflection completes the X transformation. For the X^2 transformation ($-2 \leftrightarrows 0, -1 \leftrightarrows 1$), an SPP is inserted within the MZ interferometer, adding an OAM quanta of $+2$ for even OAM modes only. A single reflection at the end completes the X^2 transformation. In the case of the $X^\dagger$ transformation ($-2 \to 1 \to 0 \to -1 \to -2$), an additional reflection is introduced within the MZ interferometer, after which an SPP subtracts one OAM quantum from the recombined modes. Finally, an additional reflection completes the $X^\dagger$ transformation. Together, the three cyclic transformations on photon B and the three phase transformations on photon A allow us to obtain all four groups of states in the four-dimensional Bell basis.

The detection system consists of a spatial light modulator (SLM), a single-mode fiber (SMF), and a single-photon detector. The SLM is used to flatten the phase of an incoming photon, transforming it into an $\ell = 0$ mode that efficiently couples to the SMF [26]. In this manner, the OAM content of single photons can be measured for specific modes or mode superpositions.

4. RESULTS

The 16 experimentally generated Bell states are analyzed using two different quantitative measures—their overlap with the theoretically expected Bell states and a witness of four-dimensional entanglement. The overlap allows us to estimate how close we are in our experiment to the ideal Bell basis, and the witness allows us to verify the presence of genuine four-dimensional entanglement in our generated states. Figure 3 shows the overlap of states within each of the four groups ψ_{0n}-ψ_{3n}. The overlap is measured by calculating the fidelity $F_{\text{exp}} = \text{Tr}(\rho_{\text{exp}}|\psi_{mn}\rangle\langle\psi_{mn}|)$, where ρ_{exp} denotes the experimentally created state and $|\psi_{mn}\rangle$ the ideal Bell states. Taking the non-flat spiral bandwidth [27] of the SPDC state into account, the maximum expected fidelity is limited to 93%. The average fidelity to the ideal state for the first group (without any cyclic transformation) is 82.1% ± 1.1%. The decrease of the measured fidelity of about 11% is mainly due to intermodal crosstalk. The other three groups combined show an average fidelity to the ideal state of 76.6% ± 2.2%. This shows that the cyclic transformation lowers the average fidelity by approximately 5.5%, which can be attributed to additional misalignments within the interferometers that comprise the X-gates.

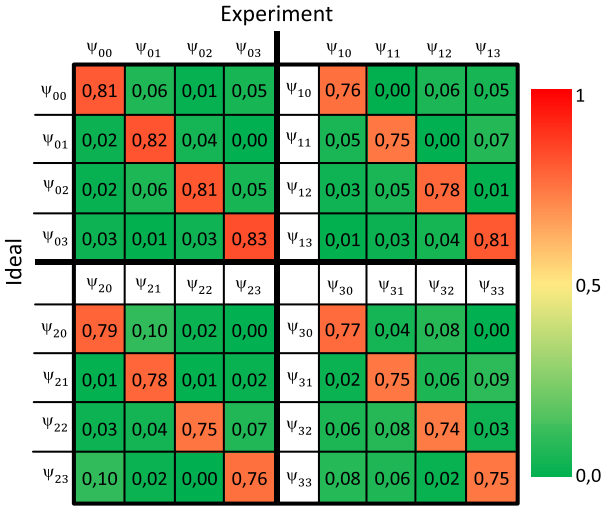

Fig. 3. Overlap between generated states and ideal Bell states. The overlap of 16 states is separated into four subgraphs as shown in the figure. The x and y axes in the figure represent the experimental and ideal Bell states, respectively. The diagonal elements indicate the fidelity F_{exp} between the experimentally generated states and the corresponding target states ψ_{mn}.

Next, we certify the entanglement dimensionality of our generated states by using a bipartite entanglement witness for d-dimensional systems [28,29]. We search for the maximal overlap of an arbitrary three-dimensional quantum state with a maximally entangled four-dimensional state (which is not necessarily a Bell state but might have different phases). The theoretical maximum overlap is $\tilde{F}_{\max} = 75\%$. If we exceed this bound in the experiment, the state is certified to be (at least) four-dimensionally entangled.

The measured fidelity witnesses F_{wit} for all 16 states are plotted in Fig. 4. Each of the 16 Bell states individually exceeds the bound of 0.75 by at least three standard deviations, and is thus certified to be four-dimensionally entangled. The error in the fidelity is calculated by propagating the Poissonian error in the photon-counting rates via a Monte Carlo simulation.

5. HIGH-DIMENSIONAL QUANTUM DENSE CODING

By replacing the SPP in our experiment with computer-generated holograms implemented on SLMs, our technique can be extended for rapidly switching between all 16 states in the four-dimensional Bell basis in an on-demand manner. This would constitute the first step in a high-dimensional quantum dense coding protocol [14]: by implementing both phase and cyclic transformations on one photon, Bob can encode 4 bits of information using the two-photon four-dimensional Bell basis. In a real application, the encoded information is lower due to crosstalk between the measured states. The experimental results of Fig. 3 lead to a mutual information of 2.6 bits (assuming that the probabilities for the not measured values, which are zero in the ideal case, are equally distributed). That exceeds the theoretical upper limit for two-dimensionally entangled states of 2 bits. The subsequent step where Alice must distinguish between all 16 Bell states in order to decode this information provides a significant challenge. It has been shown that it is impossible to unambiguously discriminate a single high-dimensional Bell state from the others with just linear optics [30]. However, it is possible to sort 16 Bell states into seven classes of states that can be distinguished with a linear optical setup, as was recently demonstrated with hyperentangled time-polarization states [31].

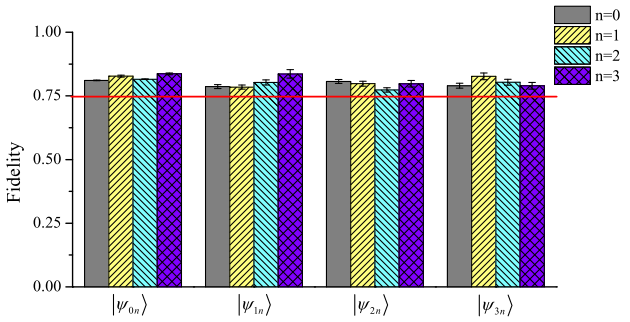

Fig. 4. Fidelity witness. Our 16 states exceed the bound for the overlap with a three-dimensionally entangled state (red line), certifying that they are all (at least) four-dimensionally entangled. The fidelity is classified into four groups ($|\psi_{0n}\rangle$, $|\psi_{1n}\rangle$, $|\psi_{2n}\rangle$, $|\psi_{3n}\rangle$) in the figure. The error is calculated using Monte Carlo simulation, and the red line denotes the theoretical bound for four-dimensional entanglement.

With linear optics only, we could therefore extract $\frac{7 \cdot 2.6}{16} = 1.14$ bits of information. However, full Bell state measurements are possible, for instance, using nonlinear optics [32].

Our experimental technique solely involves the photonic spatial degree of freedom and can thus be readily combined with well-developed techniques for polarization [33] and time-bin encoding [31], allowing for a significant increase in Hilbert space dimensionality.

6. CONCLUSION

Here we have shown the application of recently developed high-dimensional quantum gates to photonic quantum entanglement. By doing so, we were able to create a complete set of four-dimensionally entangled quantum states for which no method of creation was previously known. The quantum states we created are a high-dimensional generalization of the Bell basis, arguably the most commonly used set of entangled quantum states in two dimensions. Access to the complete high-dimensional Bell basis allows for the exploration of strong nonclassical correlations and their application in quantum information protocols such as quantum dense coding. Furthermore, our technique can be used for the generation of complete sets of high-dimensional Greenberger–Horne–Zeilinger states [6,35]. Another possible application is to create multi-qubit cluster states, which can be generated by merging several different Bell states [36]. By analogy, different types of high-dimensional multi-photon states can be produced using the technique presented here.

APPENDIX A: SUPPLEMENTARY MATERIAL

1. Deviations from the Ideal States

Deviations from the ideal states can be explained by three main effects: non-equal distribution of modes from the original state, crosstalk between modes, and loss of coherence in the interferometers. The spiral bandwidth of the OAM distribution is not flat, thus the state created in the down-conversion process is not maximally entangled. In our experiment, we measure an initial state of $|\psi\rangle = \alpha|0,0\rangle + \beta|1,1\rangle + \beta|-1,-1\rangle + \gamma|2,2\rangle$ with $\alpha/\beta = 0.69$ and $\alpha/\gamma = 0.45$. Thus the maximum possible fidelity with a maximally entangled Bell state is limited by 93%. This inherent unbalancing of the created modes can be overcome with a Procrustean filtering technique [2,37]. Another issue that lowers the fidelity is the crosstalk between different modes, and we find that in the computation basis, $\frac{\text{cross-talkcounts}}{\text{allcounts}} = 0.11(3)$. The crosstalk limits the fidelity to 91%. These impurities mainly stem from misalignments of the OAM sorter and the Mach–Zehnder interferometer, which can be reduced by active stabilization. The coherence of the off-diagonal elements in this experiment has been measured to be 0.97(6)% on average. Taking these three limiting factors into account, the expected fidelity witness values are given by $F_{\text{wit}} = 0.81(5)$. Hence, the observed average fidelity witness of $F_{\text{wit}} = 0.808 \pm 0.016$ is mainly due to unbalancing and crosstalk in the diagonal elements.

2. Overlap Between States

Here we show the data from which Fig. 3 has been created. It shows the overlap between different states from the same class, with the same OAM values but different phases.

	$\psi_{0,0}$	$\psi_{0,1}$	$\psi_{0,2}$	$\psi_{0,3}$
$\psi_{0,0}$	0,810	0,063	0,011	0,048
$\psi_{0,1}$	0,024	0,823	0,041	0,002
$\psi_{0,2}$	0,015	0,060	0,818	0,049
$\psi_{0,3}$	0,027	0,006	0,032	0,835
	$\psi_{1,0}$	$\psi_{1,1}$	$\psi_{1,2}$	$\psi_{1,3}$
$\psi_{1,0}$	0,762	0,004	0,058	0,046
$\psi_{1,1}$	0,053	0,748	0,002	0,074
$\psi_{1,2}$	0,030	0,053	0,780	0,009
$\psi_{1,3}$	0,005	0,025	0,044	0,811
	$\psi_{2,0}$	$\psi_{2,1}$	$\psi_{2,2}$	$\psi_{2,3}$
$\psi_{2,0}$	0,788	0,100	0,020	0,003
$\psi_{2,1}$	0,010	0,784	0,008	0,017
$\psi_{2,2}$	0,027	0,041	0,751	0,066
$\psi_{2,3}$	0,098	0,020	0,001	0,764
	$\psi_{3,0}$	$\psi_{3,1}$	$\psi_{3,2}$	$\psi_{3,3}$
$\psi_{3,0}$	0,773	0,042	0,076	0,003
$\psi_{3,1}$	0,022	0,745	0,056	0,089
$\psi_{3,2}$	0,055	0,076	0,740	0,031
$\psi_{3,3}$	0,076	0,061	0,018	0,747

From there, the average expected fidelity can be calculated to be $\bar{F}_{\text{exp}} = 0.78 \pm 0.03$.

3. Entanglement Witness

First, we calculate the overlap F_{wit} between our state and a d-dimensional maximally entangled target state. Then, we compute a d-dimensional entanglement bound $\mathcal{B}(d) = \sum_{\ell=0}^{d-1} \lambda_i^2$, which is the sum of the squares of all but the smallest Schmidt coefficients of the target state. If the overlap, F_{wit} exceeds the bound for a d-dimensional entangled state; then the measurement data can only be explained with a $(d+1)$-dimensionally entangled state.

4. Combining the Beams Probabilistically

In our experiments, we combine the two photon paths for photon B probabilistically. The beam splitter in Fig. 2 is implemented via a half-wave plate at 45° in the horizontal arm (after which the polarization is diagonal), and PBS. In order to erase the *which-path information*, we could use a polarizer at 45°. However, we use half-wave plate at 45°, which rotates horizontal to diagonal and vertical to anti-diagonal; afterwards we use the SLM as an effective polarizer, as the SLM only works with horizontally polarized light.

Funding. Austrian Academy of Sciences (OeAW); H2020 European Research Council (ERC) (SIQS 600645 EU-FP7-ICT); Austrian Science Fund (FWF) (SFB F40, CoQuS W1210-N16, Y879-N27); National Natural Science Foundation of China (NSFC) (11534008); Joint Czech-Austrian project MultiQUEST (I 3053-N27).

Acknowledgment. F. W. was supported by the National Natural Science Foundation of China. M. M. acknowledges support from the Austrian Science Fund (FWF) through the START project and the joint Czech–Austrian project MultiQUEST.

†These authors contributed equally to this work.

REFERENCES

1. A. Vaziri, G. Weihs, and A. Zeilinger, "Experimental two-photon, three-dimensional entanglement for quantum communication," Phys. Rev. Lett. **89**, 240401 (2002).
2. A. C. Dada, J. Leach, G. S. Buller, M. J. Padgett, and E. Andersson, "Experimental high-dimensional two-photon entanglement and violations of generalized Bell inequalities," Nat. Phys. **7**, 677–680 (2011).
3. M. Agnew, J. Leach, M. McLaren, F. S. Roux, and R. W. Boyd, "Tomography of the quantum state of photons entangled in high dimensions," Phys. Rev. A **84**, 062101 (2011).
4. D. Giovannini, J. Romero, J. Leach, A. Dudley, A. Forbes, and M. J. Padgett, "Characterization of high-dimensional entangled systems via mutually unbiased measurements," Phys. Rev. Lett. **110**, 143601 (2013).
5. M. Krenn, M. Huber, R. Fickler, R. Lapkiewicz, S. Ramelow, and A. Zeilinger, "Generation and confirmation of a (100 × 100)-dimensional entangled quantum system," Proc. Natl. Acad. Sci. USA **111**, 6243–6247 (2014).
6. M. Malik, M. Erhard, M. Huber, M. Krenn, R. Fickler, and A. Zeilinger, "Multi-photon entanglement in high dimensions," Nat. Photonics **10**, 248–252 (2016).
7. Y. Zhang, F. S. Roux, T. Konrad, M. Agnew, J. Leach, and A. Forbes, "Engineering two-photon high-dimensional states through quantum interference," Sci. Adv. **2**, e1501165 (2016).
8. S. Gröblacher, T. Jennewein, A. Vaziri, G. Weihs, and A. Zeilinger, "Experimental quantum cryptography with qutrits," New J. Phys. **8**, 75 (2006).
9. M. Mafu, A. Dudley, S. Goyal, D. Giovannini, M. McLaren, M. J. Padgett, T. Konrad, F. Petruccione, N. Lütkenhaus, and A. Forbes, "Higher-dimensional orbital-angular-momentum-based quantum key distribution with mutually unbiased bases," Phys. Rev. A **88**, 032305 (2013).
10. N. J. Cerf, M. Bourennane, A. Karlsson, and N. Gisin, "Security of quantum key distribution using d-level systems," Phys. Rev. Lett. **88**, 127902 (2002).
11. M. Huber and M. Pawłowski, "Weak randomness in device-independent quantum key distribution and the advantage of using high-dimensional entanglement," Phys. Rev. A **88**, 032309 (2013).
12. X. L. Wang, X. D. Cai, Z. E. Su, M. C. Chen, D. Wu, L. Li, N. L. Liu, C. Y. Lu, and J. W. Pan, "Quantum teleportation of multiple degrees of freedom of a single photon," Nature **518**, 516–519 (2015).
13. C. H. Bennett and S. J. Wiesner, "Communication via one-and two-particle operators on Einstein-Podolsky-Rosen states," Phys. Rev. Lett. **69**, 2881–2884 (1992).
14. K. Mattle, H. Weinfurter, P. G. Kwiat, and A. Zeilinger, "Dense coding in experimental quantum communication," Phys. Rev. Lett. **76**, 4656–4659 (1996).
15. C. H. Bennett, G. Brassard, C. Crépeau, R. Jozsa, A. Peres, and W. K. Wootters, "Teleporting an unknown quantum state via dual classical and Einstein-Podolsky-Rosen channels," Phys. Rev. Lett. **70**, 1895–1899 (1993).
16. M. Zukowski, A. Zeilinger, M. Horne, and A. Ekert, "'Event-ready-detectors,' Bell experiment via entanglement swapping," Phys. Rev. Lett. **71**, 4287–4290 (1993).
17. J. Brendel, N. Gisin, W. Tittel, and H. Zbinden, "Pulsed energy-time entangled twin-photon source for quantum communication," Phys. Rev. Lett. **82**, 2594–2597 (1999).
18. J. Leach, B. Jack, J. Romero, M. Ritsch-Marte, R. Boyd, A. Jha, S. Barnett, S. Franke-Arnold, and M. Padgett, "Violation of a Bell inequality in two-dimensional orbital angular momentum state-spaces," Opt. Express **17**, 8287–8293 (2009).
19. M. Agnew, J. Z. Salvail, J. Leach, and R. Boyd, "Generation of orbital angular momentum Bell states and their verification via accessible nonlinear witnesses," Phys. Rev. Lett. **111**, 030402 (2013).
20. L. Allen, M. W. Beijersbergen, R. Spreeuw, and J. Woerdman, "Orbital angular momentum of light and the transformation of Laguerre-Gaussian laser modes," Phys. Rev. A **45**, 8185–8189 (1992).
21. M. Krenn, M. Malik, M. Erhard, and A. Zeilinger, "Orbital angular momentum of photons and the entanglement of Laguerre-Gaussian modes," Philos. Trans. R. Soc. A **375**, 20150442 (2017).
22. M. Krenn, M. Malik, R. Fickler, R. Lapkiewicz, and A. Zeilinger, "Automated search for new quantum experiments," Phys. Rev. Lett. **116**, 090405 (2016).
23. F. Schlederer, M. Krenn, R. Fickler, M. Malik, and A. Zeilinger, "Cyclic transformation of orbital angular momentum modes," New J. Phys. **18**, 043019 (2016).

24. A. Babazadeh, M. Erhard, F. Wang, M. Malik, R. Nouroozi, M. Krenn, and A. Zeilinger, "High-dimensional single-photon quantum gates: concepts and experiments," arXiv:1702.07299 (2017).
25. J. Leach, M. J. Padgett, S. M. Barnett, S. Franke-Arnold, and J. Courtial, "Measuring the orbital angular momentum of a single photon," Phys. Rev. Lett. **88**, 257901 (2002).
26. A. Mair, A. Vaziri, G. Weihs, and A. Zeilinger, "Entanglement of the orbital angular momentum states of photons," Nature **412**, 313–316 (2001).
27. J. Torres, A. Alexandrescu, and L. Torner, "Quantum spiral bandwidth of entangled two-photon states," Phys. Rev. A **68**, 050301 (2003).
28. R. Fickler, R. Lapkiewicz, M. Huber, M. P. Lavery, M. J. Padgett, and A. Zeilinger, "Interface between path and orbital angular momentum entanglement for high-dimensional photonic quantum information," Nat. Commun. **5**, 4502 (2014).
29. M. Erhard, M. Malik, and A. Zeilinger, "A quantum router for high-dimensional entanglement," Quantum Sci. Technol. **2**, 014001 (2017).
30. J. Calsamiglia, "Generalized measurements by linear elements," Phys. Rev. A **65**, 030301 (2002).
31. A. Hill, T. Graham, and P. Kwiat, "Hyperdense coding with single photons," in *Frontiers in Optics* (2016), p. FW2B.2.
32. Y.-H. Kim, S. P. Kulik, and Y. Shih, "Quantum teleportation of a polarization state with a complete Bell state measurement," Phys. Rev. Lett. **86**, 1370–1373 (2001).
33. J. T. Barreiro, T. C. Wei, and P. G. Kwiat, "Beating the channel capacity limit for linear photonic superdense coding," Nat. Phys. **4**, 282–286 (2008).
35. M. Erhard, M. Malik, M. Krenn, and A. Zeilinger, "Experimental GHZ entanglement beyond qubits," arXiv:1708.03881 (2017).
36. P. Walther, K. J. Resch, T. Rudolph, E. Schenck, H. Weinfurter, V. Vedral, M. Aspelmeyer, and A. Zeilinger, "Experimental one-way quantum computing," Nature **434**, 169–176 (2005).
37. A. Vaziri, J. W. Pan, T. Jennewein, G. Weihs, and A. Zeilinger, "Concentration of higher dimensional entanglement: qutrits of photon orbital angular momentum," Phys. Rev. Lett. **91**, 227902 (2003).